Chemical Physics 153 (1991) 233–245
North-Holland

# Dissociative excitation of hydrogen in rf and dc glow discharges through $H_2$

S.B. Vrhovac, S.B. Radovanov, S.A. Bzenić, Z.Lj. Petrović and B.M. Jelenković
*Institute of Physics, PO Box 86, 11080 Zemun, Beograd, Yugoslavia*

Received 27 August 1990

The spectral and spatial profile of $H_\beta$ from the low pressure rf and dc glow discharges in hydrogen is studied in order to reveal the excitation mechanism of the fast excited H fragments. Measurements were performed both for the normal and abnormal dc glow discharges. Spatial distributions of the Balmer β radiation reflect the local plasma conditions in the discharge, especially the excitation efficiency which is used to determine the excitation kinetics in hydrogen discharges. Spectral $H_\beta$ profiles were measured and used to determine the kinetic energy of excited H atoms and to check which of the mechanisms describes best the results observed in our experiment. We have also calculated the number densities of vibrationally excited levels by solving a set of vibrational master equations for the conditions similar to those of our experiments, as excitation from the vibrationally excited ground-state hydrogen molecules may be used to explain the changes in the intermediate wing component of the line profile with the changing current.

## 1. Introduction

Studies of hydrogen discharges are important because it is a test case for theoretical and experimental investigations, there is still shortage of data, there are inconsistencies between different sources [1] and there is need to develop predicative models for realistic discharge conditions. Interest in hydrogen or hydrogen/hydrocarbon discharges has recently increased because of its importance in production of amorphous and crystalline carbon films [2]. In fusion research, studies of $H_2$ are related to fundamental knowledge of the breakdown, diagnostic and neutral beam production [3]. In microelectronics pure $H_2$ and its mixtures are used for selective etching of InP, GaAs, InGaAsP, AlGaAs and thin oxide films and cleaning of silicon or metallic surfaces [4]. Kinetics of hydrogen collisions are of interest in the development of fast high-current switches such as thyratrons [5] and finally it is worth mentioning that spectroscopy of hydrogen is used in diagnostics of nitrading discharges [6] and of the earth's atmosphere [7].

Dissociative excitation is one of the dominant processes in gas discharges, both as an important dissociation channel or as a source of easily detectable Balmer radiation which can be used for diagnostics. In experiments with monoenergetic electron beams dissociation dynamics of the hydrogen molecule is studied through the analysis of Doppler profiles of the hydrogen Balmer lines. Here, Doppler broadened Balmer lines reflect the mechanism of excited hydrogen atom production [8–12] and it is possible to obtain their kinetic energy distribution. The energy distribution function (EDF) of excited hydrogen atoms produced in $e–H_2$ collisions usually consist of a "slow group", with a maximum in the 0–2 eV region, and of a "fast group" with a distribution peaking at 7–8 eV. There are numerous combinations of final states of fragments with channels that open above 16.6 eV, mostly in the 26–40 eV region [13]. The maximum energy that is shared between two fragments does not exceed 40 eV [14].

Hydrogen line shapes in glow discharges show line widths which exceed by far the thermal Doppler widths and their structure is different from the profiles obtained in the electron beam experiments. This was confirmed by the measurements of Balmer line shapes done in dc [15–18] and rf [18–20] discharges. The line profiles obtained in dc experiments

show wide wings which indicate the presence of excited hydrogen atoms with remarkably high energies (100 eV). These "far" wings correspond to energies much larger than those of the "fast group" (as obtained from the beam experiments) whose contribution will be labeled here as "intermediate wings". Several mechanisms were proposed to explain the far wings. Those include dissociative excitation by ions, desorption and subsequent excitation of particles from the surface, dissociative recombination and excitation and neutralization of incident ions by collisions with surface [17–21]. Even the so called intermediate wings in gas discharges have energies larger than what can be expected on the basis of potential energy diagrams. Sultan and co-workers [20] gave an alternative explanation for the intermediate wings ($\epsilon \simeq 50$ eV) observed in their experiment. They propose that the desorption of vibrationally excited $H_2$ from the electrode surface enhances the high-energy electron impact excitation in the sheath region and is responsible for the production of every fast fragments.

The mean kinetic energy of the fast atom differs greatly in different discharge conditions, electrode geometry, observation angle and is usually evaluated from the fwhm of the line profile and not from the kinetic energy distribution. Therefore there are still ambiguities in both the explanation of the excitation mechanism and evaluating procedure. Spatial profiles of both dc and rf discharges proved to be very useful tests of discharge models and gave indication of the mean energy of electrons and indirectly of the mechanism of energy deposition [22–25]. Makabe and co-workers [25] made extensive comparisons with their numerical model of temporally and spatially resolved $H_\alpha$ emission from $H_2$ discharge.

In this paper the Balmer β line profiles in rf (27.12 MHz) and dc glow discharges are used to study the kinetic energy distribution (EDF) of the product atoms. We also measured the spatial distribution of $H_\beta$ radiation along the *E*-field direction. The measurements were done at different pressures, currents and voltages and at several positions in the discharge. Kinetics of dissociative excitation in the sheath and in the bulk of the discharge is distinctly different so such measurements can give us information on the relative importance of different mechanisms. As our results for small (2 mA) and large (20 mA) currents gave quite different spectral profiles we attempt to establish the correlation between the non-equilibrium population of vibrationally excited molecules [26] which provide a possibility of opening new channels for dissociative excitation. Therefore, we have calculated the vibrational level population from $v=0$–13 of the ground-state hydrogen molecule for two electron concentrations, to see if the distribution function of the vibrational population could play an important role in the formation of the fast atom fragments.

## 2. Experiment

The apparatus used in this work has been described in our previous publication [23] and will be discussed only briefly.

The discharge was operated in a stainless steel chamber with two parallel plate electrodes with a diameter of 60 mm and an electrode gap of 20 mm. The rf power is applied from a 27 MHz generator through an impedance matching network and is monitored by a standard rf power meter. The current and voltage were measured throughout the experiment. The typical incident power was 60 W, with the peak to peak voltage 500–800 V and a bias voltage of about 125 V.

The dc measurements were done with the electrode set placed in a glass tube in order to prevent breakdown towards the wall of the vacuum chamber. The discharge current was 2 mA in the normal glow regime and 20 mA in the abnormal glow regime, while the discharge voltages were 330 and 1200 V, respectively. In both cases the discharge was diffuse.

The gas density used in the experiments ranged from $3\times10^{15}$–$1.8\times10^{16}$ cm$^{-3}$ (0.1–0.6 Torr). Flow rates were between 5–10 sccm and were controlled with an MKS model 258B mass flow controller. The pressure was determined to better than 1% and the flow rates to 0.5%.

Balmer radiation emitted from the glow discharge was observed through a quartz window mounted on the stainless steel vacuum chamber. The observation angle was perpendicular to the discharge axis. An optical scanning system was used in order to resolve the light spatially with a resolution of 0.5 mm. The monochromator was a SPEX 1802 with a dispersion of 0.4 nm/mm. Normally a 30 μm slit was used. The resolution was tested by using the 434.7 nm Hg line

and the fwhm obtained was 0.02 nm. Single photons were detected with a cooled photomultiplier (EMI 6256) and counted by a photon counting chain.

## 3. Results and discussion

### 3.1. Spatial profiles

The optical emission spatial profiles obtained from rf discharge at two different pressures are shown in figs. 1a, b. These profiles are usually not symmetric to the mid-point of the discharge axis, since the system is asymmetric. The observed differences in spatial dependencies of $H_\beta$ radiation, between rf- and dc-field (see figs. 1 and 2.) at the same pressure are significant. These differences reflect the changes in the electron density and energy distribution function, field distribution and consequently excitation efficiency in both discharges.

In rf glow discharge (figs. 1a, b) the position of the brightest region is strongly dependent on the pressure. At lower pressure (0.1 Torr) in the rf field the region of very high $E/N$ (where $E$ is the electric field and $N$ is the gas number density) and low collision frequency is extended. This is similar to what Bletzinger and De Joseph [22] found in $N_2$/Ar rf discharges and we found in $N_2$ rf discharges [23]. On the basis of the spatial profile of emission at lower pressure one cannot distinguish between the "wave riding" and the "secondary electron" mechanisms [27]. However, development of the sharp peak at 0.4 Torr indicates the "secondary electron" mechanism of power deposition into the discharge [27]. At higher pressure electron multiplication in the cathode fall may be expected to be larger and thus contribute to the observed spatial profile.

The electron density in the rf field is rather low in the electrode vicinity so the maximum of excitation is shifted towards the larger distances compared to dc discharges (figs. 2a, b) as found by Kushner [28].

The spatial profiles in the dc glow discharge with the glass tube placed around the electrodes were rather similar to those obtained without it. Significant difference between the spatial profiles for the normal and abnormal glow (discharges were diffuse in both cases) is in the relative intensity of the negative glow as compared to the "bulk" of the discharge. In the nor-

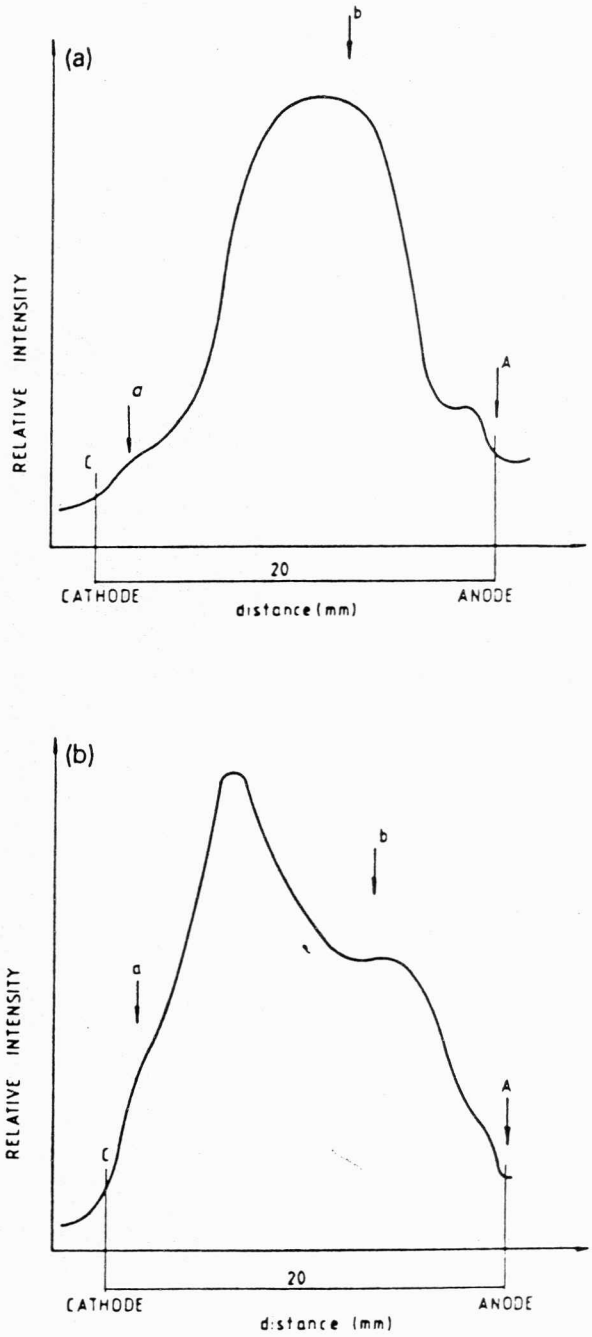


Fig. 1. (a) Spatial profile of Balmer β radiation in rf glow discharge at 0.1 Torr. Spectral profiles were taken at points labelled a and b. (b) Spatial profile of Balmer β radiation in rf glow discharge at 0.4 Torr.

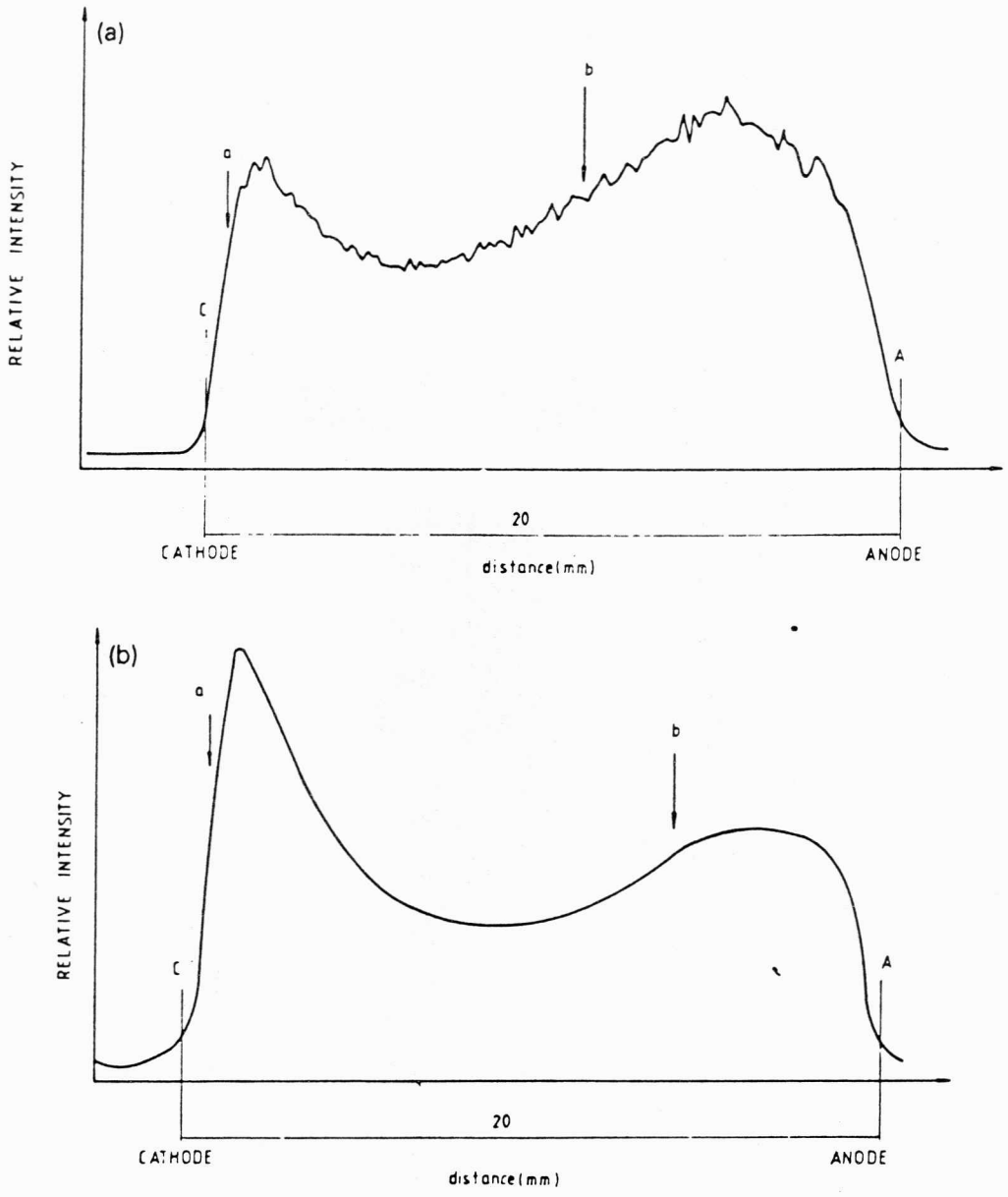


Fig. 2. (a) Spatial profile of Balmer β radiation in normal dc glow discharge at 0.6 Torr ($I=2$ mA; $U=330$ V). (b) Spatial profile of Balmer β radiation in abnormal dc glow discharge at 0.4 Torr ($I=20$ mA; $U=1200$ V).

mal glow discharge the intensity of radiation from the negative glow is not significantly larger than the intensity from the bulk. The intensity of radiation from the negative glow is significantly increased for the "abnormal glow" discharge (fig. 2b).

### *3.2. Spectral line shapes and kinetic energy distribution of H**

#### *3.2.1. Analysis of line profiles*

The product hydrogen atoms in dc and rf discharges, are in the excited states H($n$) and decay into lower states, resulting in the emission of photons. By

looking at these photons, more precisely by observing the Doppler profiles, the velocity and kinetic energy distributions of the product atoms can be found.

The experimental profile of Balmer lines is the convolution of Doppler profile and instrumental width since collisional broadening, fine structure (fwhm $\simeq 0.0077$ nm for $H_\beta$) and Stark effect (fwhm $\simeq 0.0028$ nm at $n_e \simeq 10^{10}$ cm$^{-3}$ for $H_\beta$) are negligible [29]. The Balmer line profile usually consists of a narrow central peak and wings. However, one has to be aware of the neighbouring molecular lines. In rf discharge two weak features of the molecular radiation were obtained on both wings of Balmer β profile and another one further towards the red side of the spectrum (see fig. 3a). These features were subtracted from the $H_\beta$ line assuming the symmetry of the atomic line.

The observable emission profile $I(\lambda)$ of the Balmer radiation is related to the true Doppler profile $I_d(\lambda')$ and the instrumental profile $I_i(\lambda-\lambda')$ by a convolution integral:

$$I(\lambda) = \int I_d(\lambda')\, I_i(\lambda-\lambda')\, d\lambda' . \qquad (1)$$

In order to solve this integral equation it was necessary to apply the Gaussian fitting procedure. We considered the instrumental profile as a single Gaussian and an experimental one as a sum of Gaussians of different halfwidths. Under these assumptions the given integral equation is equivalent to a system of linear algebraic equations. In this way the Gaussian coefficients of the deconvoluted profile $I_d(\lambda')$ were evaluated and the full Doppler profile was obtained. Following Ogawa and Higo [10,30], we have calculated the translational energy distribution $\Pi(\epsilon)$ of excited hydrogen $H^*(n=4)$ atoms by differentiating the full Doppler shape:

$$\Pi(\epsilon) = -\frac{\text{const.} \times dI(\lambda)}{d\lambda} . \qquad (2)$$

$$\epsilon = \tfrac{1}{2} mc^2 \left(\frac{\lambda-\lambda_0}{\lambda_0}\right)^2 \cong 19.85(\lambda-\lambda_0)^2 , \qquad (3)$$

where $\epsilon$ is the energy in eV, $m$ the atom mass, $c$ the light velocity, $\lambda$ is the wavelength in Å and $\lambda_0$ the wavelength at the center of the line. Eq. (2) is valid only when the anisotropy of dissociation and optical emission can be neglected. For the conditions of our measurements, it is justified to assume that the anisotropy of dissociative excitation by electrons is small [11]. To check for small instrumental asymmetries of the profiles, the EDF was obtained from both halfs of the profile separately and compared. Following this procedure the kinetic energy distribution of fragments was obtained for each experimental profile.

From the half width of the line the non-thermal average kinetic energy can be derived. The mean kinetic energy of atoms obtained in this way is often used by different authors to discuss the mechanism of the dissociative excitation. However, this value, obtained by different formulae in the single energy approximation, is misleading since the realistic kinetic energy distribution functions cannot be easily approximated by either a delta function or a Maxwellian function [31]. Even when the bulk of the distribution can be described by a Maxwellian distribution the high energy tail cannot be. So the kinetic energy distribution is in principle the most desirable one for understanding the excited molecular state dissociation.

The measurements of the Balmer line profiles have shown that for different discharge conditions profiles can differ greatly. We have measured the $H^*$ energy distribution in rf discharge at 0.1 and 0.4 Torr and in dc discharge at 0.4–0.6 Torr. Profiles were usually obtained at two positions, near the electrode (sheath) and in the mid gap (bulk). Points at which the spectral scans were taken are shown on scans of spatial dependence of emitted radiation (figs. 1 and 2).

### 3.2.2. *Balmer β profile in rf glow discharge in $H_2$*

Typical profiles obtained for $H_\beta$ in the sheath and in the bulk of the rf discharge in pure $H_2$ at 0.1 Torr and the corresponding kinetic energy distributions are presented in figs. 3a,b. The profiles exhibit a central, nearly Gaussian shape peak (with fwhm of 0.06 nm in the bulk and 0.08 nm in the sheath) due to the velocity distribution of the slow hydrogen atoms. The kinetic energy distributions in both cases show a single slow component which falls rapidly with an average energy of 0.22 eV for the bulk of the discharge and of 0.3 eV for the sheath. This narrow peak is attributed mainly to the atoms produced by the dissociation of the Rydberg states ($1s\sigma$) ($nl$) converging to the $^2\Sigma_g^+$ ($1s\sigma_g$) state of $H^+$ and predissociation of vibrationally excited states such as the $1s\sigma_g$ state (see

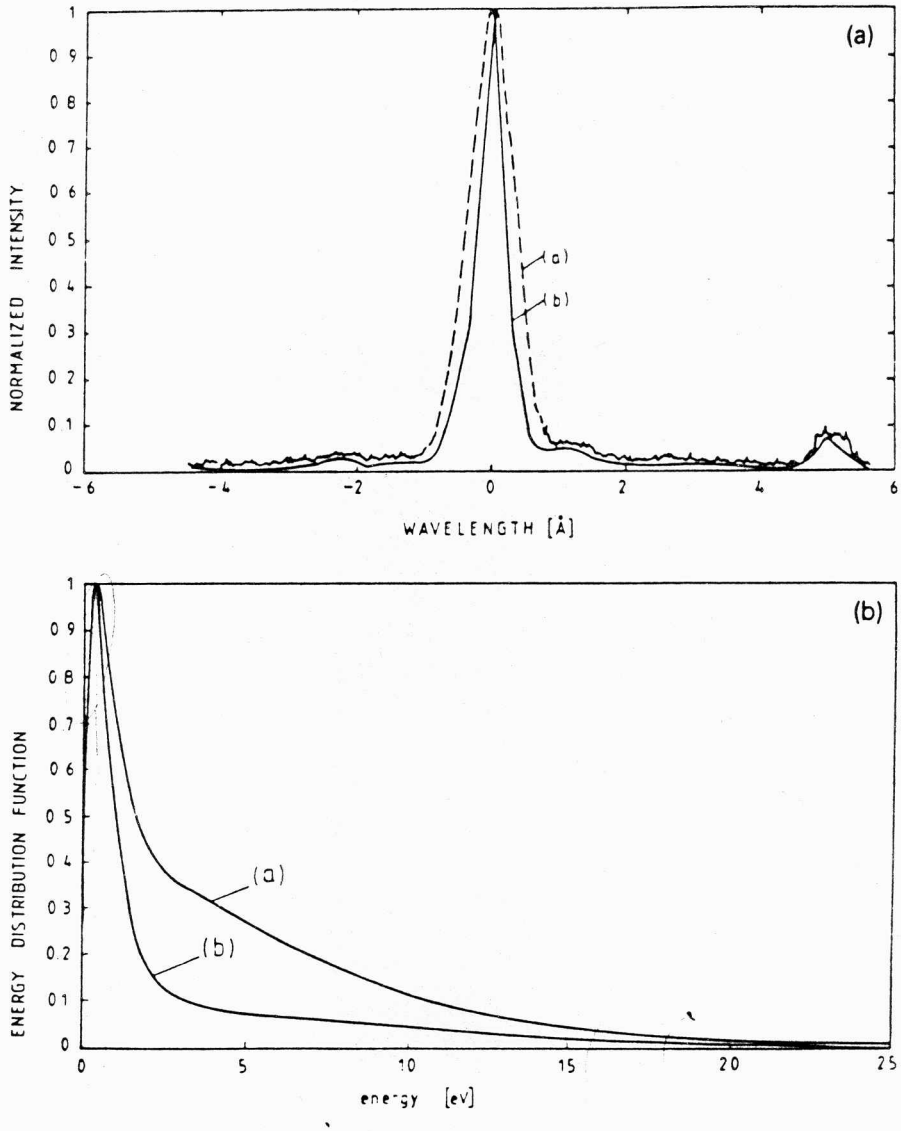


Fig. 3. (a) The Doppler profiles of Balmer β line observed in rf glow discharge at 0.1 Torr; (a) sheath, (b) bulk. (b) Kinetic energy distribution function of H($n=4$) atoms in rf discharge: (a) sheath, (b) bulk.

fig. 4.). The threshold energy for these processes is 17 eV.

The kinetic energy distribution, obtained in the sheath of the rf discharge, indicates the existence of H* atoms with relatively higher energies (4–10 eV). These atoms can be produced through the repulsive low lying doubly excited states converging to the $^2\Sigma_u^+(2p\sigma)$ of $H^+$. Schiavone and co-workers [9] suggested the $^1\Sigma_u^+(2p\sigma_u)^2$ to be the most important for the production of 4 eV hydrogen atoms, since this state is the lowest doubly excited state in the Franck–Condon region around 26 eV. Higher doubly excited states of ($2p\sigma_u$, $nl\lambda$) series which cross the middle of the Franck–Condon region, below the first excited $H_2^+$ state ($2p\sigma_u$), dissociate to H($nl$) – + H(1s) and contribute to the 8 eV hydrogen atoms [32]. Few of these ($2p\sigma_u$, $nl\lambda$) states, at large internuclear distances, cross the Rydberg series ($1s\sigma_g$, $nl\lambda$) converg-

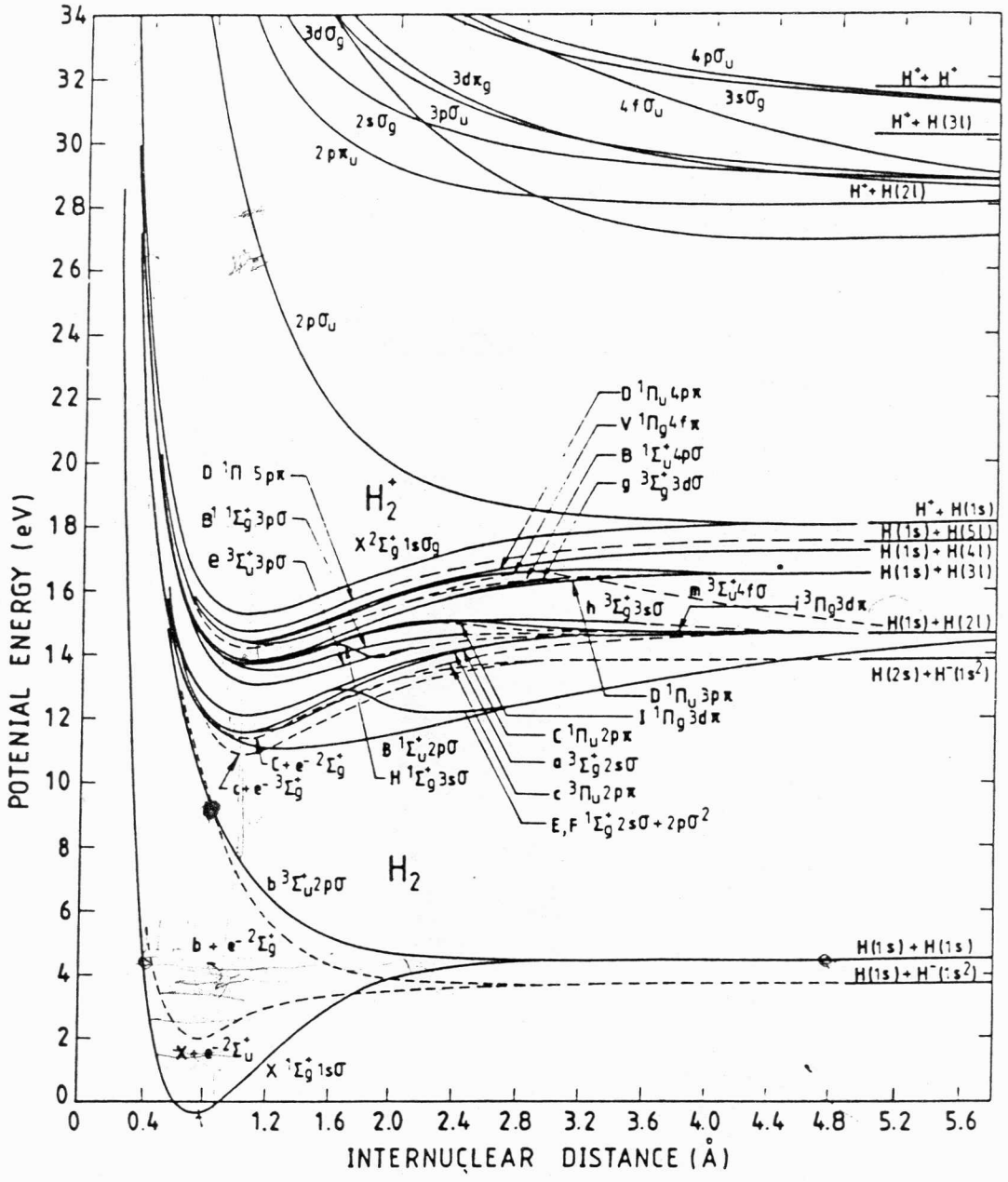


Fig. 4. Potential energy curves for $H_2$ and $H_2^+$ (from Sharp [14]).

ing to $H_2^+$ ($1s\sigma_g$) state and consequently lead to fragments of the same energy.

The energy distributions obtained in the sheath and in the bulk of the discharge when compared with beam experiment distributions indicate that the number of higher energy electrons (above 26 eV) is significantly increased in the sheath.

The line profiles obtained in hydrogen rf discharge at 0.4 Torr are rather similar to those measured at 0.1 Torr, while the spatial distributions of Balmer β ra-

diation are quite different. In the sheath the lines are somewhat broader and the structure of the intermediate wings changes in the same manner at both pressures. Identical mechanism of excitation at two pressures indicates that the significantly different spatial profiles (figs. 1a, b) are due to a different spatial distribution of electron density and not due to a different power deposition mechanism.

*3.2.3. Balmer β profile in dc glow discharge in $H_2$*

In figs. 5 and 6 the line profiles measured in the sheath (a) and in the bulk (b) of the dc discharge at 2 and 20 mA are shown. The corresponding kinetic energy distributions are given in fig. 7. In the bulk of the normal and abnormal glow discharge the identical EDF was evaluated. The slow component has a mean energy of 0.2 eV and the fast component has a mean energy of 8 eV which is in agreement with the

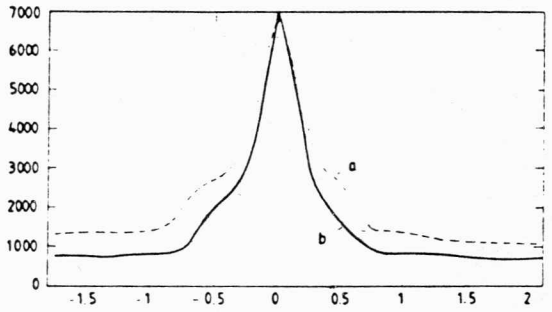


Fig. 5. Doppler profiles of the Balmer β line observed in normal glow discharge: curve a in the sheath, curve b in the bulk.

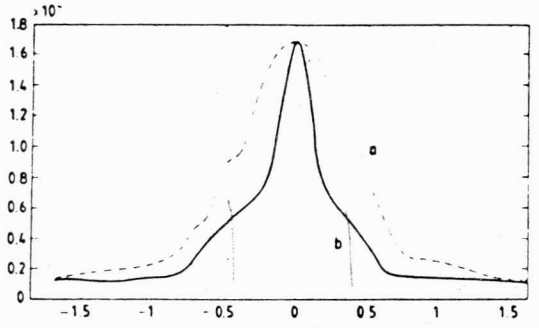


Fig. 6. The Doppler profiles of the Balmer β line observed in the dc abnormal glow discharge: curve a in the sheath, curve b in the bulk.

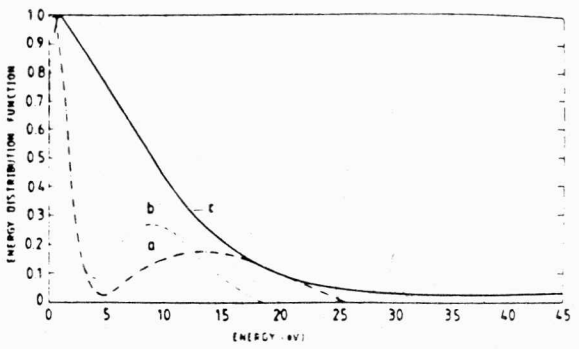


Fig. 7. Kinetic energy distribution function of H ($n=4$) fragment atoms in dc glow discharge: curve a in the sheath of the normal glow, curve b in the bulk of the normal glow and curve c in the sheath of the abnormal glow.

results obtained using beam experiments [10]. Both the low and high energy components are thought to be created through the same excited states of $H_2$ as discussed already for spectral profiles in rf discharges. In the sheath of the normal glow discharge a similar EDF was derived but with a tail extended to somewhat higher energies. The shift towards higher energies of the maximum in the EDF, in the sheath region, can be attributed to the existence of vibrationally excited molecules which collide with higher energy electrons producing the emissive fragment with large kinetic energy. The shift and shaping of the EDF of the product H* ($n=4$) atoms, obtained in this experiment, correspond fairly well with the shaping theoretically obtained by Celiberti and co-workers [33] when vibrationally excited ground state molecules are taken into account. These calculations were done for different electron energies showing that differences in the cross sections for the process $H_2(X\,^1\Sigma_g^+,\ v=0\text{–}13)+e \rightarrow H(n=1)+H(n=4)+e$ determine the intensity of the EDF.

In the sheath of the abnormal glow a broad EDF was evaluated with the main peak at 1 eV and a very high energy tail up to 45 eV. These changes can be connected with the nonequilibrium vibrational distribution too, because nonequilibrium vibrational distribution with increased current density further modifies the high energy tail of the EDF. However, the observed changes in the intensity and shaping of the EDF, in the sheath of the abnormal glow, can also be due to heavy particle collisions, as expected for

very high values of $E/N$ in the sheath of the abnormal glow [21].

Our preliminary measurements of the Balmer β Doppler shift, in the direction of the electric field (observed through one of the electrodes) of the abnormal glow discharge, have shown that high energy H* atoms with mean energies in excess of 100 eV exist in the same experimental conditions as discussed here. From the measured line profile it was found that a significant number of atoms are moving towards the cathode as well away from the cathode with energies of the order of 100 eV which is in agreement with the results of Benesch and Li [15]. A significant contribution to the line wings may come from the fast ions and neutrals and these effects were studied in more detail by Petrovic and co-workers [21]. By comparing the model of hydrogen low-current discharge [1] to experimental data these authors found that at high $E/N$ values such as those found in cathode fall of glow discharges electron excitation in the cathode vicinity is less important. Petrovic and co-workers [21] found that the dominant excitation of Balmer lines comes from the collisions of fast $H_2$ and H which may excite molecular hydrogen into H*. Ions hitting the surface may get neutralized and reflected back as excited atoms with high kinetic energy. Fast back reflected excited atoms may contribute to the wings in "side on" measurements if scattered at an angle different from 90°. The flux of outgoing excited atoms was found to depend strongly on the surface materials [15.21] and stainless steel has one of the largest yields of excited atoms.

As suggested by Sultan et al. [16] and shown in these measurements, the electron impact of vibrationally excited molecules may also lead to high energy of fragments. This mechanism which is dominant in the bulk region will be analyzed in more detail in the following section.

### 3.3. Population of vibrationally excited levels

The strong dependence on the current of the Doppler profiles in dc glow discharges indicates that excitation from highly excited vibrational levels could be rather important. Therefore we have performed calculations of the vibrational level population of the ground state hydrogen molecule directed towards interpreting the line profiles and discussing the importance of vibrationally excited molecules in the formation of kinetic energy distribution of slow and fast hydrogen atoms.

A well-know fact is that the direct dissociation cross sections are affected by the vibrational excitation. This was confirmed by the calculations of several authors where they present the dependence of electron cross section on the vibrational quantum number and show that the increase of vibrational energy decreases the threshold energy of the electron impact dissociation processes [33–35]. As mentioned above (see section 3.2.3.) the nonequilibrium vibrational distribution deeply affects the kinetic energy distribution (EDF) of the hydrogen atoms and protons [33] generated by direct dissociative excitation and/or ionization mechanisms.

In this section we will briefly discuss the influence of different processes on the vibrational level population. In particular the present results are applied to the bulk experimental situation in the discharge. To integrate the system of vibrational master equations we have used a software package, PLOD, which is based on the Gear stiff formulas.

Nonequilibrium vibrational kinetics can be modeled provided one takes into account the following points [36–44]:

(a) Low energy electrons are responsible for direct excitation of lower vibrational levels. (e–V) while the higher vibrational states ($v' = 5$–$14$) are populated mainly through resonant excitation via singlet states (E–V).

(b) Vibrational excitation is reduced or enhanced (depending on the quantum number) through collisions of two vibrationally excited molecules in the vibrational–vibrational (V–V) energy transfer. Such non-resonant vibrational energy exchange increases the population of upper energy levels.

(c) The vibrational population is also determined by the vibrational–translational (V–T) energy transfer. It is worth mentioning that the de-excitation (V–T) rate ($v \rightarrow v-1$) increases monotonically with vibrational quantum number and is important for $v > 6$ [35–37].

(d) We have estimated the electron density for the normal glow to be $1 \times 10^{10}$ cm$^{-3}$. For such discharge conditions ($T_g = 300$ K, $p = 0.4$–$0.6$ Torr, $n_e \simeq 1 \times 10^{10}$ cm$^{-3}$) the rates for atomic–molecular collisions which lead to vibrational de-excitation are compara-

bly smaller than the V–T rates. Furthermore, the concentration of atoms is sufficiently small compared to the molecules since the degree of ionization and dissociation is small ($10^{-4}$–$10^{-5}$) in rf and dc glow discharges with current density up to $10^{-4}$ A/cm$^2$ [37,47]. Judging by the kinetic equations, provided that there is no loading and the recombination is negligible, the electron number density may be expected to be proportional to the current.

The vibrational master equations system can be writen in general form as:

$$\frac{\partial N_\nu}{\partial t} = \left(\frac{\partial N_\nu}{\partial t}\right)_{e-V} + \left(\frac{\partial N_\nu}{\partial t}\right)_{e-V} + \left(\frac{\partial N_\nu}{\partial t}\right)_{V-V} + \left(\frac{\partial N_\nu}{\partial t}\right)_{V-T} . \quad (4)$$

Explicit expressions for these terms have been reported previously [35–40].

The corresponding excitation and relaxation processes were incorporated into the vibrational master equation. It should be noticed that e–V processes start from ground the vibro-electronic state of the $H_2$ molecule and that rotational excitation and termalization effects of electron–electron interactions have not been included in these calculations. The rotational excitation is important in the case of lower $E/N$ than those considered in this experiment. Basically we have solved the system of vibrational master equations describing the temporal evolution of the population density of the fourteen vibrational levels of $H_2$, starting with all molecules in the level $\nu=0$ at time $t=0$ in the flow regime. The rate coefficients for e–V energy exchange were taken from Buckman and Phelps [45] and for V–V and V–T processes from Cacciatore et al. [40] and Biling and Fisher [46].

Fig. 8 shows the relative population of the excited vibrational levels $N_\nu(\nu)$ compared to the ground vibrational level for two electron densities at 30 Td. The low value of $E/N$ was chosen to be able to compare our results with other available calculations. In case of cathode sheaths a much higher $E/N$ would be expected. Yet even in that case one may expect a good correspondence between current and electron number density.

It can be seen that populations fall rapidly with increasing vibrational quantum number (for $n_e=10^{10}$ cm$^{-3}$) because of the declining e–V pumping rates

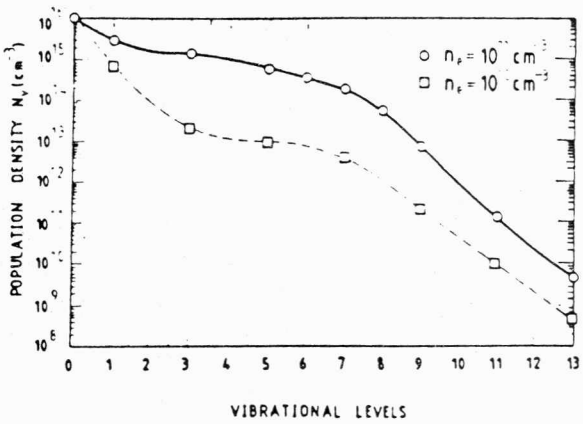


Fig. 8. Populations of vibrationally excited levels in $H_2$ at 5 ms.

[36]. For lower vibrational levels $\nu<5$ the e–V rates are dominant. However, at the upper end of the vibrational spectrum the e–V rates are small compared with the E–V and V–T rates, and the relative contributions to successive levels decline is slower for E–V than for e–V processes. Moreover, at the upper end of the vibrational ladder the populations are depleted by V–T de-excitation following E–V formation. At intermediate levels we observed a characteristic plateau on the vibrational distribution which is more pronounced when approaching the quasi stationary conditions ($t=10^{-2}$ s). Also the V–T losses are small compared to high e–V and V–V rates, which is true for hydrogen at low gas temperatures and low pressures.

The calculations were extended to the population via electronic excitation of C $^1\Pi_u$ state which affects particularly the population of higher vibrational levels. No significant difference was noticed when the B $^1\Sigma_u$ state was included in the calculation. This is in accordance with the transition moments of both states and the fraction $F(B,\nu'')$ as evaluated by Hiskes and co-workers [37,38]. We have also noticed that the obtained distribution with de-excitation processes for $t=10^{-2}$ s is similar to the one calculated without recombination processes.

The present calculation shows that high populations of vibrationally excited molecules may be expected in discharges under conditions that lead to the observation of the high energy excited hydrogen atoms. Furthermore, with increased electron density ($n_e=10^{11}$ cm$^{-3}$) the number of vibrationally excited

molecules in higher vibrational levels ($v > 5$) is increased. Such changes in the vibrational distribution influence the kinetic energy distribution of the product hydrogen atoms (EDF) in the manner that the difference between distinct regions of low and higher energy atoms in the EDF is slowly disappearing.

## 4. Summary

In the present paper we have reported a study of spatial dependence of emitted $H_\beta$ radiation and of the kinetic energy distribution of hydrogen atoms in dc and rf field discharges at various points along the field axis.

In particular we have shown the importance of vibrationally excited molecules affecting the EDF in the bulk and in the sheath of the glow discharges. The correlation was made between experimentally obtained changes in the EDF with the changes in the vibrational distribution induced by increased current.

The $H_\beta$ profiles measured in the rf glow discharge and the corresponding single component EDF with a tail up to 25 eV proved that the electron impact dissociative excitation playa a key role in the mechanism of excited hydrogen atom production. No essential difference has been notices between the sheath and the bulk of the rf discharge at 0.1 and 0.4 Torr which implicates that the excitation mechanism in both cases is the same though it does not exclude a possible directed component of heavy particles. In dc normal and abnormal glow discharge the two component EDF was obtained in the bulk region, thus indicating that electron impact excitation determines the excitation mechanism in the bulk region through (1) the predissociation of vibrational excited states or Rydberg states directly dissociated leading to the production of slow hydrogen atoms or (2) repulsive doubly excited states leading to the production of fast hydrogen atoms. In the sheath region of the normal glow, the shift of the maximum in the EDF towards higher energies was evaluated and attributed to the existence of the emissive H* higher energy fragments which are formed in the collisions of the vibrationally excited molecules with the higher energy electrons.

In the sheath region of the abnormal dc glow discharge the single component EDF was evaluated. The high energy tail of EDF is greatly enhanced and extended up to 45 eV. Our recent measurements of Balmer β Doppler shift, in the direction of the electric field, in similar experimental conditions, have shown that high energy H* atoms with energies up to 500 eV exist in the cathode fall region of the abnormal glow. We have also noticed the presence of back-scattered H* atoms with energies up to 100 eV. These atoms are preferentially produced in heavy particle collisions (i.e. in the gas phase charge exchange collisions and ion or neutral surface collisions) where vibrationally excited molecules play a significant role. Further experimental studies are in progress in order to reveal the importance of heavy particle collisions for the fast atom production.

## Acknowledgements

Authors in this paper are grateful to Dr. A.V. Phelps for comments on the manuscript. The work reported here was partially funded by the Science Foundation of Serbia and by the USA–Yugoslav Joint Fund for scientific collaboration, projects JF 926 and 924 (administered by NIST).

## References

[1] A.V. Phelps, J. Phys. Chem. Ref. Data. 19 (1990) 653;
M.A. Morrison, R.W. Crompton, Bidhan Saha and Z.Lj. Petrović, Australian J. Phys. 40 (1987) 239.

[2] A.B. Harker and J.F. DeNatale, J. Mater. Res. 5 (1990) 818;
M. Kamo, Y. Sato, S. Matsumoto and N. Setaka, J. Cryst. Growth. 62 (1983) 642;
S. Matsumoto, Y. Sato, M. Kamo and N. Setaka, Japan J. Appl. Phys. 21 (1982) L 183;
S. Matsumoto, Y. Sato and T. Tsutsumi, J. Mater. Sci. 17 (1982) 3106;
W.C. Roman, M.B. Colkett, S.O. Hayand and C.A. Eckbreth, ISPC-9, Pugnochiuso, Italy, 9th Intern. Symp. Plasma Chem. (1989) L82;
I. Watanabe and K. Sugata, Japan J. Appl. Phys. 27 (1988) 1397;
R. Meilunas, M.S. Wong, K.C. Sheng, R.P.H. Chang and R.P. Van Duyne, Appl. Phys. Letters 54 (1989) 2204;
F.G. Celii, P.E. Pehrsson, H.T. Wang and J.E. Butler, Appl. Phys. Letters 54 (1988) 2043.

[3] S. Yoshida, H. Sugai and H. Toyoda, Japan J. Appl. Phys. 28 (1989) 1101;
K. Kondo, K. Okazaki, T. Oda, N. Noda, K. Akiashi, H.

molecules in higher vibrational levels ($v > 5$) is increased. Such changes in the vibrational distribution influence the kinetic energy distribution of the product hydrogen atoms (EDF) in the manner that the difference between distinct regions of low and higher energy atoms in the EDF is slowly disappearing.

## 4. Summary

In the present paper we have reported a study of spatial dependence of emitted $H_\beta$ radiation and of the kinetic energy distribution of hydrogen atoms in dc and rf field discharges at various points along the field axis.

In particular we have shown the importance of vibrationally excited molecules affecting the EDF in the bulk and in the sheath of the glow discharges. The correlation was made between experimentally obtained changes in the EDF with the changes in the vibrational distribution induced by increased current.

The $H_\beta$ profiles measured in the rf glow discharge and the corresponding single component EDF with a tail up to 25 eV proved that the electron impact dissociative excitation playa a key role in the mechanism of excited hydrogen atom production. No essential difference has been notices between the sheath and the bulk of the rf discharge at 0.1 and 0.4 Torr which implicates that the excitation mechanism in both cases is the same though it does not exclude a possible directed component of heavy particles. In dc normal and abnormal glow discharge the two component EDF was obtained in the bulk region, thus indicating that electron impact excitation determines the excitation mechanism in the bulk region through (1) the predissociation of vibrational excited states or Rydberg states directly dissociated leading to the production of slow hydrogen atoms or (2) repulsive doubly excited states leading to the production of fast hydrogen atoms. In the sheath region of the normal glow, the shift of the maximum in the EDF towards higher energies was evaluated and attributed to the existence of the emissive H* higher energy fragments which are formed in the collisions of the vibrationally excited molecules with the higher energy electrons.

In the sheath region of the abnormal dc glow discharge the single component EDF was evaluated. The high energy tail of EDF is greatly enhanced and extended up to 45 eV. Our recent measurements of Balmer β Doppler shift, in the direction of the electric field, in similar experimental conditions, have shown that high energy H* atoms with energies up to 500 eV exist in the cathode fall region of the abnormal glow. We have also noticed the presence of back-scattered H* atoms with energies up to 100 eV. These atoms are preferentially produced in heavy particle collisions (i.e. in the gas phase charge exchange collisions and ion or neutral surface collisions) where vibrationally excited molecules play a significant role. Further experimental studies are in progress in order to reveal the importance of heavy particle collisions for the fast atom production.

## Acknowledgements

Authors in this paper are grateful to Dr. A.V. Phelps for comments on the manuscript. The work reported here was partially funded by the Science Foundation of Serbia and by the USA–Yugoslav Joint Fund for scientific collaboration, projects JF 926 and 924 (administered by NIST).

## References

[1] A.V. Phelps, J. Phys. Chem. Ref. Data. 19 (1990) 653;
M.A. Morrison, R.W. Crompton, Bidhan Saha and Z.Lj. Petrović, Australian J. Phys. 40 (1987) 239.

[2] A.B. Harker and J.F. DeNatale, J. Mater. Res. 5 (1990) 818;
M. Kamo, Y. Sato, S. Matsumoto and N. Setaka, J. Cryst. Growth. 62 (1983) 642;
S. Matsumoto, Y. Sato, M. Kamo and N. Setaka, Japan J. Appl. Phys. 21 (1982) L 183;
S. Matsumoto, Y. Sato and T. Tsutsumi, J. Mater. Sci. 17 (1982) 3106;
W.C. Roman, M.B. Colkett, S.O. Hayand and C.A. Eckbreth, ISPC-9, Pugnochiuso, Italy, 9th Intern. Symp. Plasma Chem. (1989) L82;
I. Watanabe and K. Sugata, Japan J. Appl. Phys. 27 (1988) 1397;
R. Meilunas, M.S. Wong, K.C. Sheng, R.P.H. Chang and R.P. Van Duyne, Appl. Phys. Letters 54 (1989) 2204;
F.G. Celii, P.E. Pehrsson, H.T. Wang and J.E. Butler, Appl. Phys. Letters 54 (1988) 2043.

[3] S. Yoshida, H. Sugai and H. Toyoda, Japan J. Appl. Phys. 28 (1989) 1101;
K. Kondo, K. Okazaki, T. Oda, N. Noda, K. Akiashi, H.

Kaneko, T. Mizuuchi, F. Sano, O. Motojima and A. Iiyoshi, Japan J. Appl. Phys. 27 (1988) 2368;
M. Bacal, Physica Scripta T2/2 (1982) 467;
P.J. Eenshuistra, M. Gochitashvilli, R. Becker, A.W. Kleyn and H.J. Hopman, J. Appl. Phys. 67 (1990) 85;
J.R. Hiskes, A.M. Karo and P.A. Willmann, J. Appl. Phys. 58 (1985) 1759.

[4] S.J. Pearton and W.S. Hobson, J. Appl. Phys. 66 (1989) 5009 and 5018;
T. Minami, T. Miyata, A. Iwamoto, S. Takata and H. Nanto, Japan J. Appl. Phys. 27 (1988) L1753;
T.R. Hayes, M.A. Dreisbach, P.M. Thomas, W.C. Dautremouth-Smith and L.A. Heimbrook, J. Vac. Sci. Technol. B 7 (1989) 1130.4;
B. Anthony, L. Breaux, T. Hsu, S. Banerjee and A. Tasch, J. Vac. Sci. Technol. B 7 (1989) 621;
B. Tomčik, S. Radovanov, Z. Petrović and B. Jelenković, Plasma Treatment of Metalic Surfaces: Improvement of Ohmic contact conductivity, Proc. VIII ISPC, Tokyo (1987) 1726;
B. Anthony, L. Breaux, T. Hsu, S. Banerjee and A. Tasch, J. Vac. Sci. Technol. B 7 (1989) 621.

[5] M.J. Kushner, J. Appl. Phys. 63 (1988) 2532.

[6] L. Petitjean and A. Ricard, J. Phys. D 17 (1984) 919.

[7] R.P. Rohrbaugh, B.A. Tinsley, H. Rassoul, Y. Sahai, N.R. Teixeira, R.G. Tull, D.R. Ross, A.L. Cochran, W.D. Cochran and E.S. Barker, J. Geophys. Res. 88 (1983) 6317.

[8] K. Ito, N. Oda, Y. Hatano and T. Tsuboi, Chem. Phys. 17 (1976) 35;
K. Ito, N. Oda, Y. Hatano and T. Tsuboi, Chem. Phys. 21 (1977) 203.

[9] R.S. Freund, J.A. Schiavone and D.F. Brader, J. Chem. Phys. 64 (1976) 1122;
D.E. Donohue, J.A. Schiavone and R.S. Freund, J. Chem. Phys. 67 (1977) 769;
R.S. Freund, D.E. Donohue and G.J. Fisanick, J. Chem. Phys. 80 (1984) 1754;
J.A. Schiavone, K.C. Smith and R.S. Freund, J. Chem. Phys. 63 (1975) 1043.

[10] T. Ogawa and M. Higo, Chem. Phys. Letters 63 (1979) 610;
K. Nakashima and T. Ogawa, J. Chem. Phys. 83 (1985) 4920;
T. Ogawa and M. Higo, Chem. Phys. 52 (1980) 55;
M. Higo, S. Kamata and T. Ogawa, Chem. Phys. 66 (1982) 243;
K. Nakashima, H. Tomura and T. Ogawa, Chem. Phys. Letters 138 (1987) 575.

[11] T. Ogawa, M. Taniguchi, K. Nakashima, H. Kawazumi, Chem. Phys. 137 (1989) 323.

[12] I. Nishiyama, T. Kondow and K. Kuchitsu, Chem. Phys. Letters 68 (1979) 333.

[13] C. Karolis and E. Harting, J. Phys. B 11 (1978) 357;

[14] T.E. Sharp, At. Data 2 (1971) 119.

[15] W. Benesch and E. Li, Opt. Letters 9 (1984) 338.

[16] G. Sultan, G. Baravian, M. Gantois, G. Henrion, H. Michel and A. Richard, Chem. Phys. 123 (1988) 423.

[17] E. Li Ayers and W. Benesch, Phys. Rev. A 37 (1988) 194.

[18] S.B. Vrhovac, S.B. Radovanov, Z.Lj. Petrović and B.M. Jelenković, in: Proc. XIX ICPIG, ed. J. Labat (Belgrade, 1989) p. 410; Proc. 9th Intern. Symp. Plasma Chem., ed. R. d'Agostino (Pignochiuso, 1989) p. 597.

[19] A.L. Cappeli, R.A. Gottscho and T.A. Miller, Plasma Chem. Plasma Processing 5 (1985) 317.

[20] G. Baravian, Y. Chouan, A. Richard and G. Sultan, J. App. Phys. 61 (1987) 5249.

[21] Z.Lj. Petrović and A.V. Phelps, submitted to ESCAMPIG 90;
Z.Lj. Petrović, B.M. Jelenkovic and A.V. Phelps, unpublished.

[22] B. Bletzinger and C.A. DeJoseph Jr., IEEE Trans. Plasma Sci. 14 (1986) 124.

[23] S.B. Radovanov, B. Tomčik, Z.Lj. Petrovic and B.M. Jelenkovic, J. Appl. Phys. 67 (1990) 97.

[24] N. Mutsukara, K. Kobayaschi and Y. Machi, J. Appl. Phys. 66 (1989) 4688.

[25] T. Kokubo, F. Tochikubo and T. Makabe, J. Phys. D 22 (1989) 1281;
K. Okazaki, T. Makabe and Y. Yamaguchi, Appl. Phys. Letters 54 (1989) 1742;
N. Goto and T. Makabe, J. Phys. D 23 (1990) 686.

[26] C. Gorse, M. Capitelli and A. Richard, J. Chem. Phys. 82 (1985) 1900.

[27] Ph. Belenguer and J.P. Boeuf, Phys. Rev. 41 (1990) 4447.

[28] M.J. Kushner, J. Appl. Phys. 53 (1982) 2939; ibid., 54 (1983) 4958; ibid., 63 (1988) 2532.

[29] R.S. Freund, J.A. Schiavone and D.F. Brader, J. Chem. Phys. 64 (1976) 1122.

[30] J. Kurawaki and T. Ogawa, Chem. Phys. 86 (1984) 295;
T. Ogawa, private communication.

[31] M.D. Tasić, Z.Lj. Petrović and J.M. Kurepa, Chem. Phys. 134 (1989) 163.

[32] A.M. Hazi, J. Phys. B 8 (1975) L262;
C. Bottcher, J. Phys. B 7 (1974) L352.

[33] R. Celiberto, M. Cacciatore, M. Capitelli and C. Gorse, Chem. Phys. 133 (1989) 355; ibid., 133 (1989) 369;
R. Celiberto, M. Capitelli and M. Cacciatore, Chem. Phys. 140 (1990) 209.

[34] J.N. Bardsley and J.M. Wadhera, Phys. Rev. 20 (1979) 1398.

[35] J.R. Hiskes, Comments At. Mol. Phys. 19 (1987) 1398.

[36] C. Gorse, M. Capitelli, M. Bacal, J. Bretagne and A. Lagana, Chem. Phys. 117 (1987) 177.

[37] J.R. Hiskes, J. Appl. Phys. 56 (1984) 1927;
J.R. Hiskes, A.M. Karo, M. Bacal, M. Brunteau and W.G. Graham, J. Appl. Phys. 53 (1982) 3469.

[38] J.R. Hiskes and A.M. Karo, Production and Neutralization of Negative Ions and Beams, 3rd Intern. Symp., Brookhaven, AIP Conf. Proc. 111 (1983) p. 3.

[39] C. Gorse, M. Capitelli, J. Bretagne and M. Bacal, Chem. Phys. 93 (1985) 1.

[40] M. Cacciatore, M. Capitelli, S. DeBenedictis, M. Dilonardo and C. Gorse, in: Non-equilibrium Vibrational Kinetcs, ed. M. Capitelli (Springer, Berlin, 1986).

[41] M. Capitelli and E. Molinari, in: Topics in Current Chemistry 90, Plasma Chemistry II (Springer, Berlin, 1980).
[42] M. Cacciatore, M. Capitelli and C. Gorse, J. Phys. D 13 (1980) 575.
[43] M. Cacciatore, M. Capitelli and M. Dilonardo, Chem. Phys. 34 (1978) 193.
[44] M. Capitelli, M. Dilonardo and E. Molinari, Chem. Phys. 20 (1977).
[45] S. Buckman and A.V. Phelps, JILA Information Report, 1985.
[46] G. Billing and E. Fisher, Chem. Phys 18 (1976) 225.
[47] J. Loureiro and C.M. Ferreira, J. Phys. D 22 (1989) 1680.